Supporting Information

Formation of Disk- and Stacked Disk-Like Self-Assembled Morphologies from Cholesterol-Functionalized Amphiphilic Polycarbonate Diblock Copolymers[§]

Shrinivas Venkataraman [a], Ashlynn L. Lee [a], Hareem T. Maune [b], James L. Hedrick [b], Vivek M. Prabhu [c], and Yi Yan Yang [a*]*

[a] Institute of Bioengineering and Nanotechnology, 31 Biopolis Way, The Nanos, Singapore 138669, Singapore

[b] IBM Almaden Research Center, 650 Harry Road, San Jose, CA 95120, USA

[c] Materials Science and Engineering Division, Materials Measurement Laboratory, National Institute of Standards and Technology, 100 Bureau Drive, Gaithersburg, MD 20899-8541

[*] **Corresponding authors:**

Tel: 1-301-975-3657; Fax: 1-301-975-3928; Email: vprabhu@nist.gov

Tel: 65-6824-7106; Fax: 65-6478-9084; E-mail: yyyang@ibn.a-star.edu.sg

Materials and methods‡

Materials

Unless, specifically mentioned, all materials were purchased from Sigma-Aldrich or TCI and all other solvents were of analytical grade, purchased from Fisher Scientific or J. T. Baker and used as received. Macroinitiator, mPEG-OH (5.0 kDa) was purchased from Polymer Source Inc., Canada. Trimethylene carbonate (TMC) was purchased from Boehringer Ingelheim (Ingelheim, Germany) and was dried extensively by freeze-drying under high vacuum. 1,8-Diazabicyclo[5.4.0]undec-7-ene (DBU) was distilled from CaH_2 under dry N_2 and transferred to a glove box. *N*-(3,5-Trifuluoromethyl)phenyl-*N*′-cyclohexylthiourea (TU) catalyst[1] was prepared as described elsewhere. Before transferring into the glove box, monomers and other reagents (like mPEG-OH) were dried extensively by freeze-drying under high vacuum.

Methods

Nuclear magnetic resonance (NMR) spectroscopy

The ^{1}H- and ^{13}C-NMR spectra of monomers and polymers were recorded using a Bruker Avance 400 spectrometer, and operated at 400 and 100 MHz respectively, with the solvent proton signal as the internal reference standard.

Molecular weight determination by size exclusion chromatography (SEC)

SEC was conducted using THF as the eluent for monitoring the polymer conversion and also for the determination of polystyrene equivalent molecular weights of the macro-transfer agents. THF-SEC was recorded on a Waters 2695D (Waters Corporation, USA)

Separation Module equipped with an Optilab rEX differential refractometer (Wyatt Technology Corporation, U.S.A.) and Waters HR-4E as well as HR-1 columns (Waters Corporation, USA). The system was equilibrated at 30 °C in THF, which served as the polymer solvent and eluent with a flow rate of 1.0 mL/min. Polymer solutions were prepared at a known concentration (ca. 3 mg/mL) and an injection volume of 100 μL was used. Data collection and analysis were performed using the Astra software (Wyatt Technology Corporation, USA; version 5.3.4.14). The columns were calibrated with series of polystyrene standards ranging from M_p = 360 Da to M_p = 778 kDa (Polymer Standard Service, USA).

Determination of critical association concentration (CAC)

The CAC values of the polymers in de-ionized (DI) water were determined by fluorescence spectroscopy using pyrene as the probe. The fluorescence spectra were recorded by an LS 50B luminescence spectrometer (Perkin Elmer, U.S.A.) at 25 °C. The polymer samples were equilibrated for 10 min before taking measurements. Aliquots of pyrene in acetone solution (6.16×10^{-5} M, 10 μL) were added to glass vials and air-dried to remove the acetone. Polymer solutions of varying concentrations were added to the pyrene at 1 mL each and left to stand for 24 h. The final pyrene concentration in each vial is 6.16×10^{-7} M. The excitation spectra were scanned at excitation wavelength from 300 to 360 nm with an emission wavelength of 395 nm. Both the excitation and emission bandwidths were set at 2.5 nm. The intensity (peak height) ratio of I339/I334 from the excitation spectra was analyzed as a function of polymer concentration. The CAC was

taken at the point of intersection between the tangent to the curve at the inflection and tangent of the points at low concentrations.

General method for determining the kinetics of polymerization

In a 7 mL vial containing a magnetic stir bar, in glove box, Chol-MTC (150 mg, 243 μmol, 10.0 equivalents), TU (9.0 mg, 24.3 micromoles, 1.0 equiv.) were dissolved in dichloromethane (1.0 mL). To this solution, was (-) S (5.6 μL, 5.7 mg, 24.3 μmol, 1.0 equiv.) added. After stirring the reaction mixture for about 5 min, Bn-CH_2OH (2.5 μL, 2.6 mg, 24.3 μmol, 1.0 equiv.) was added to initiate polymerization. The reaction mixture was allowed to stir at room temperature and aliquots of samples were taken to monitor the monomer conversion and the molecular weight by ^1H NMR spectroscopy and SEC. Typically aliquots (~ 80 μL) were removed from the reaction vial and immediately quenched with benzoic acid solution (1.0 mg/mL concentration in CH_2Cl_2, ~ 80 μL). Monomer conversions were determined by comparing the integral values of resonances of a singlet ($\delta = 0.75 - 0.55$ ppm) corresponding to one of the CH_3- protons in both the cholesterol monomer and the resultant polymer *versus* doublet ($\delta = 4.80 - 4.60$ ppm) arising from CH_2O(C=O)O corresponding to the residual monomer at that kinetic time point. Monomer conversion at a given time *t* is calculated as follows:

$$\text{Percentage monomer conversion} = ((1-[M]_t)/[M]_0)*100$$

$$= ((1 - (\text{Int}_{4.80 \text{ to } 4.60}/2) / (\text{Int}_{0.75 \text{ to } 0.55}/3))*100$$

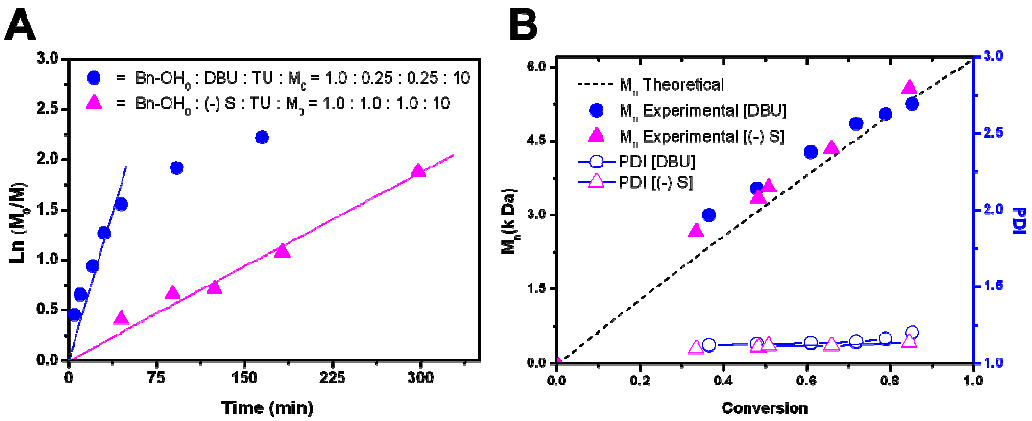

Figure S1. (**A**) Semi-logarithmic kinetic plot for the OC-ROP of monomer **3** using different catalyst systems, $[\text{Bn-OH}]_0$: DBU : TU : $[\mathbf{3}]_0$ = 1.0 : 0.25 : 0.25 : 10 (filled circle) and $[\text{Bn-OH}]_0$: (-) S : TU : $[\mathbf{3}]_0$ = 1.0 : 1.0 : 1.0 : 10 (filled triangle); (**B**) Evolution of experimental M_n (filled symbols) and PDI (open symbols) as a function of monomer conversion for $[\text{Bn-OH}]_0$: DBU : TU : $[\mathbf{3}]_0$ = 1.0 : 0.25 : 0.25 : 10 (circle) and $[\text{Bn-OH}]_0$: (-) S : TU : $[\mathbf{3}]_0$ = 1.0 : 1.0 : 1.0 : 10 (triangle). Evolution of theoretical M_n is depicted by dotted line.

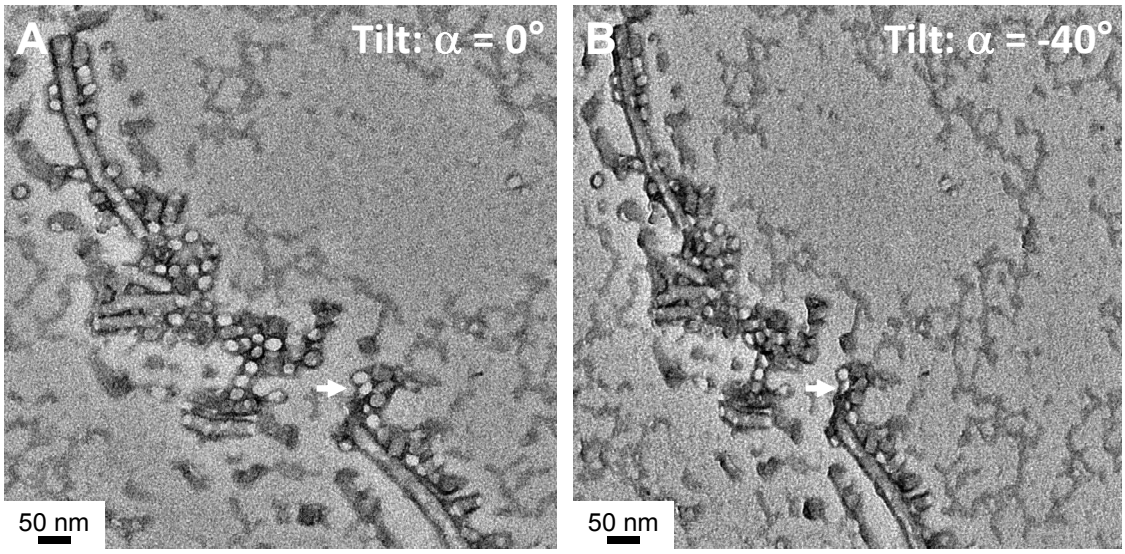

Figure S2. TEM images of polymer **5b** obtained (**A**) without tilt (α = 0°) and (**B**) with tilting (tilt α = - 40°) of the stage by an angle respectively, demonstrating that circular structures upon tilting appeared as ellipsoidal structures (or *vice versa*).

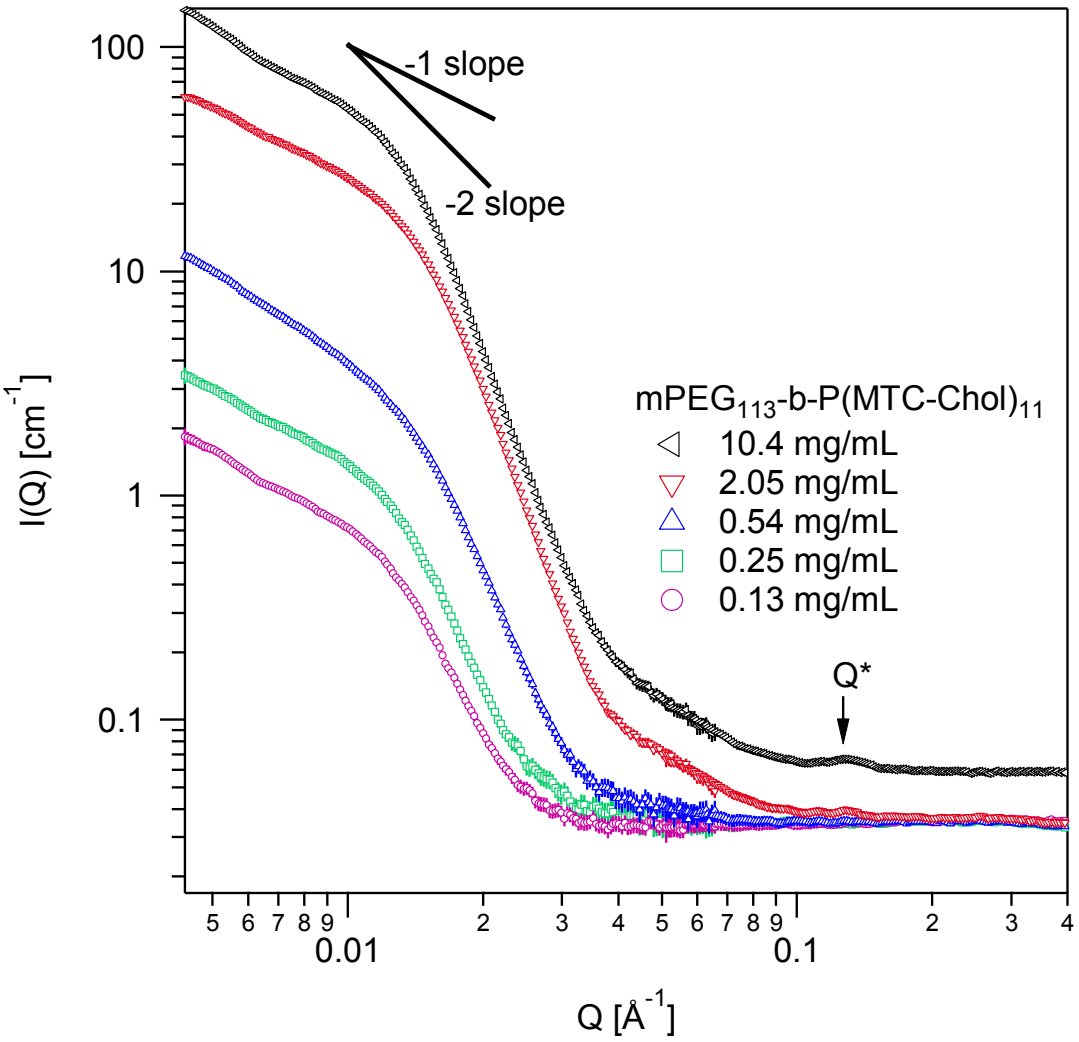

Figure S3. SANS from $mPEG_{113}$-*b*-$P(MTC\text{-}Chol)_{11}$ in deuterium oxide at five prepared concentrations. A broad peak is identified, Q*, at the highest 2 concentrations.

Summary of Pedersen model for block copolymer scattering with power law.

In the model fitting approach the Pedersen theory for scattering by block copolymer micelles [2, 3] is used in conjunction with a power law contribution to account for the additional larger shapes observed via TEM or associative behavior without excessive parameterization. Secondly, the power law contribution appears experimentally in the low-Q region at length scales larger than the expected micelles. Equation 1 is fit to the SANS data as a function of scattering vector Q, where A and B are prefactors related to the concentration of species and Δ is the power law index. I_{inc} is a Q-independent incoherent background. The structural parameters that quantify the micelle, described below, are within the F_{mic} form factor.

$$I(Q) = AQ^{-\Delta} + B\,F_{mic}(Q) + I_{inc} \qquad (1)$$

The form factor of the micelle, F_{mic}, contains four correlation terms: a self-correlation of the disk core (F_d), the self-correlation of corona chains (F_c), the cross-correlation between chain and core (S_{dc}), and cross-correlation between different chains (S_{cc}) leading to the following equation,

$$F_{mic}(Q) = N^2\beta_d^2 F_d(Q) + N^2\beta_c^2 F_c(Q) + 2N^2\beta_d\,\beta_c\,S_{dc}(Q) + N(N-1)\beta_c^2 S_{cc}(Q) \qquad (2)$$

N is the aggregation number of block copolymers in a micelle and β_d and β_c are the total excess scattering length of a block in the disk core and chain corona, respectively. They are defined by $\beta_d = V_d(\rho_d - \rho_{solv})$ and $\beta_c = V_c(\rho_c - \rho_{solv})$, where V_d and V_c are

the volumes of a block in the core and corona, respectively. ρ_d, ρ_c, and ρ_{solv} are the scattering length densities of the disk core, corona chains, and solvent, respectively.

The first term in Eq. (2) is the form factor for the disk core of radius R and thickness L with self-correlation,

$$\mathbf{F_d}(Q,R,L) = \int_0^{\frac{\pi}{2}} \Psi(\mathbf{Q},\mathbf{R},\mathbf{L},\boldsymbol{\alpha})^2 \sin\alpha \, d\alpha \qquad (3)$$

Where, the analytic expression for the amplitude $\Psi(Q,R,L,\alpha)^2$ is given by

$$\Psi(Q,R,L,\alpha)^2 = \frac{[2B_1(\mathbf{QRsin}]\,\alpha)}{\mathbf{QRsin}\,\alpha} \frac{\sin\left(\frac{\mathbf{QL}\cos\alpha}{2}\right)}{\frac{\mathbf{QL}\cos\alpha}{2}} \qquad (4)$$

and B_1(x) is the first-order Bessel function of the first kind. The square of the amplitude is numerically integrated over all orientation angles α.

The second term in Eq. (2) is the form factor of the Gaussian chain given by the Debye structure factor, Eq, where $\mathbf{x} = Q^2 R_g^2$. The radius of gyration of the polymer chain in the corona is given by R_g.

$$\mathbf{F_c(Q)} = \frac{2[\mathbf{e}^{-\mathbf{x}} - \mathbf{1} + \mathbf{x}]}{\mathbf{x}^2} \qquad (5)$$

The third term in Eq. (2) is the cross-correlation between chain and core, Eq. 6, whereby the Gaussian chains are uniformly distributed at d×R_g away from the surface of the core upon a coaxial cylinder of radius R + d×R_g. d is used to parameterize the non-penetration of corona chains with the core when d is close to unity.

$$S_{dc}(Q) = \varphi(QR_g) \int_0^{\frac{\pi}{2}} \Psi(Q,R,L,\alpha)\,\Xi(Q,R+dR_g,L+2dR_g,\alpha)\sin\alpha\, d\alpha \qquad (6)$$

Where the form factor for the amplitude of the shell is:

$$\Xi(Q,R,L,\alpha) = \left[\frac{\frac{R}{R+L}\frac{[2B_1(QR\sin\alpha)}{QR\sin\alpha}\cos\left(\frac{QL\cos\alpha}{2}\right) + \frac{L}{R+L}B_0(QR\sin\alpha)\sin\left(\frac{QL\cos\alpha}{2}\right)}{\frac{QL\cos\alpha}{2}}\right] \qquad (7)$$

B_0 is the zeroth order Bessel function of the first kind. The first term represents the contribution from the circular ends of the disk and the second from the edges, each contribution is weighted by the relative surface area. $\varphi(x) = \frac{[1-e^{-x}]}{x}$ is the form factor amplitude for the Gaussian chain. Since the chain is isotropic, it does not depend of the orientation angle.

The last term in Eq. 2 is the interference term between the corona chains as given by the orientation average of the shell form factor squared multiplied by the single chain form factor amplitude squared.

$$S_{cc}(Q) = \varphi^2(QR_g) \int_0^{\frac{\pi}{2}} \Xi(Q, R + dR_g, L + 2dR_g, \alpha)^2 \sin\alpha \, d\alpha \quad (8)$$

Pedersen fit details

The MTC-Chol segments that comprise the disk-core and PEG corona have scattering length densities of ρ_d = 7.78 10^{-7} Å^{-2} and ρ_c = 5.92 10^{-7} Å^{-2}, respectively, calculated as the sum of the atomic scattering lengths (b_i within a molecular volume (v), such that $\rho = \sum b_i / v$. The contrast for scattering arises from scattering length density difference between the blocks and solvent, deuterium oxide (ρ_{solv} = 6.33 10^{-6} Å^{-2}) in this case. In order to reduce the fit parameter uncertainty, the 3 data sets of different concentration were globally fit with common disk core parameter values R,L with fixed ρ_d, ρ_c, ρ_{solv}, and R_g whereas the prefactor A, Δ, B, and I_{inc} were allowed to be free parameters for each of the 3 SANS datasets. The volume per MTC-Chol block was estimated as V_d = 11236 Å^3 and the volume per PEG block volume was taken as $V_c = 4\pi R_g^3/3$, after Pedersen, where R_g was estimated by $R_g = 0.215\ M_w^{0.583}$ [Å].[4] The micelle aggregation number (N) is determined by the ratio of the core volume (with radius R and thickness L) to the volume per block in the core and includes a parameter for solvent content within the core [3]. However, since the solutions had some sediment the true concentration is not known and remains a fit parameter, which is a direct product to the scattering prefactors and makes them correlated to the solvent content. The fit result are shown in **Table 1S**.

Table S1. Fit results for power law and Pedersen model to mPEG$_{113}$-*b*-P(MTC-Chol)$_4$

Conc. [mg/mL]	*B*	*R* [nm]	*L* [nm]	*A*	Δ	I_{inc} [cm^{-1}]

0.2	$(6.46 \pm 0.1)10^{-12}$			$(2.43 \pm 0.3)10^{-14}$	2.60± 0.02	0.0341± 0.0001
2.5	$(5.24 \pm 0.06)10^{-11}$	7.15 ± 0.02	3.77 ± 0.03	$(2.98 \pm 0.01)10^{-13}$	2.50± 0.007	0.0558± 0.0002
10.4	$(4.17 \pm 0.04)10^{-10}$			$(2.26 \pm 0.02)\ 10^{-12}$	2.44 ±0.002	0.0405± 0.0002

Model Independent Fits

The average micelle cross-section can be estimated by a Guinier-like limiting law where the form of the scattering follows $Q \times I \approx \exp(-Q^2 R^2_{g,c}/2)$ for cylindrically-symmetric objects [5]. On a plot of $\ln[Q/(Q)]$ versus Q^2 the slope provides $R^2_{g,c}/2$, where $R_{g,c}$ is the cross sectional radius of gyration. The cross-sectional radius of the equivalent solid object is related to the radius of gyration by $R = \sqrt{2}\ R_{g,c}$. The limiting law plots for $mPEG_{113}$-b-$P(MTC\text{-}Chol)_4$ and $mPEG_{113}$-b-$P(MTC\text{-}Chol)_{11}$ are shown in **Figure 4Sa and 4Sb**. The main results are shown in **Table 2S** and **3S**.

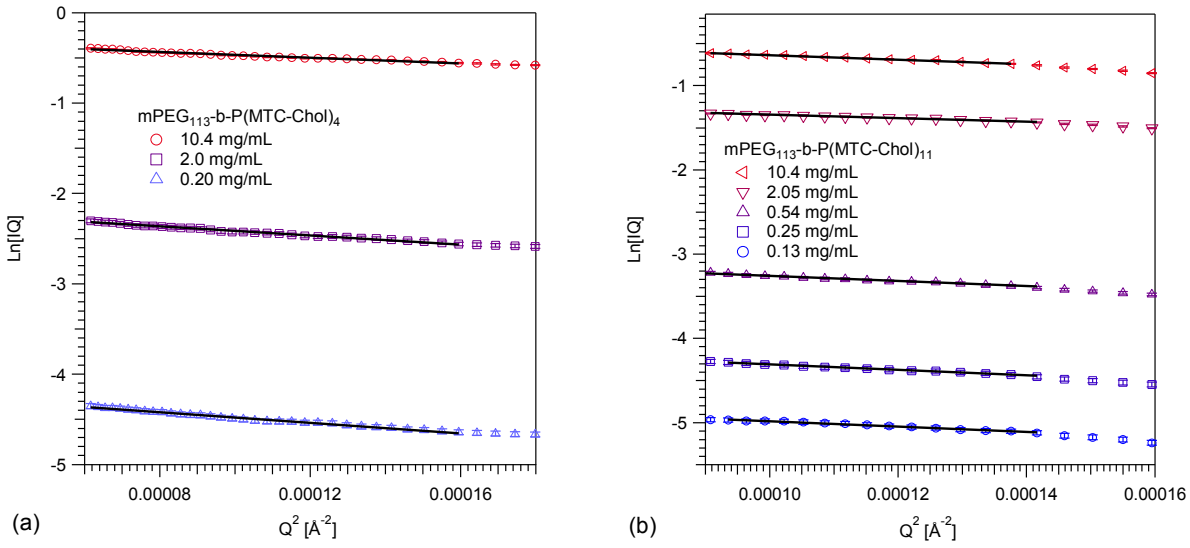

Figure 4S. Plot to estimate the cross-section radius of gyration ($R_{g,c}$) for (**a**) $mPEG_{113}$-*b*-$P(MTC\text{-}Chol)_4$ and (**b**) $mPEG_{113}$-*b*-$P(MTC\text{-}Chol)_{11}$. This model-independent approach is consistent with TEM values for the radius.

Table S2. mPEG$_{113}$-*b*-P(MTC-Chol)$_4$ model-independent cross section

C [mg/mL]	*model independent*	*model independent*
Sample	R_g cross section [nm]	$D = 2\sqrt{2}\ R_g$ [nm]
0.2	9.35 ± 0.25	26.4 ± 0.3
2.5	8.70 ± 0.2	24.6 ± 0.6
10.4	6.85 ± 0.1	19.4 ± 0.3
average*	8.3 ± 1.3	23.5 ± 3.6

* ± 1 standard deviation from the mean.

Table S3. mPEG$_{113}$-*b*-P(MTC-Chol)$_{11}$ model-independent cross section

C [mg/mL]	*model independent*	*model independent*
Sample	R_g cross section [nm]	$D = 2\sqrt{2}\ R_g$ [nm]
0.13	11.4 ± 0.8	32.2 ± 2.3
0.25	11.45 ± 0.8	32.4 ± 2.3
0.54	11.10 ± 0.15	31.4 ± 0.4
2.05	8.95 ± 0.2	25.3 ± 0.6
10.4	10.35 ± 0.2	29.3 ± 0.6
Average*	10.65 ± 1.0	30.1 ± 3.0

* ± 1 standard deviation from the mean.

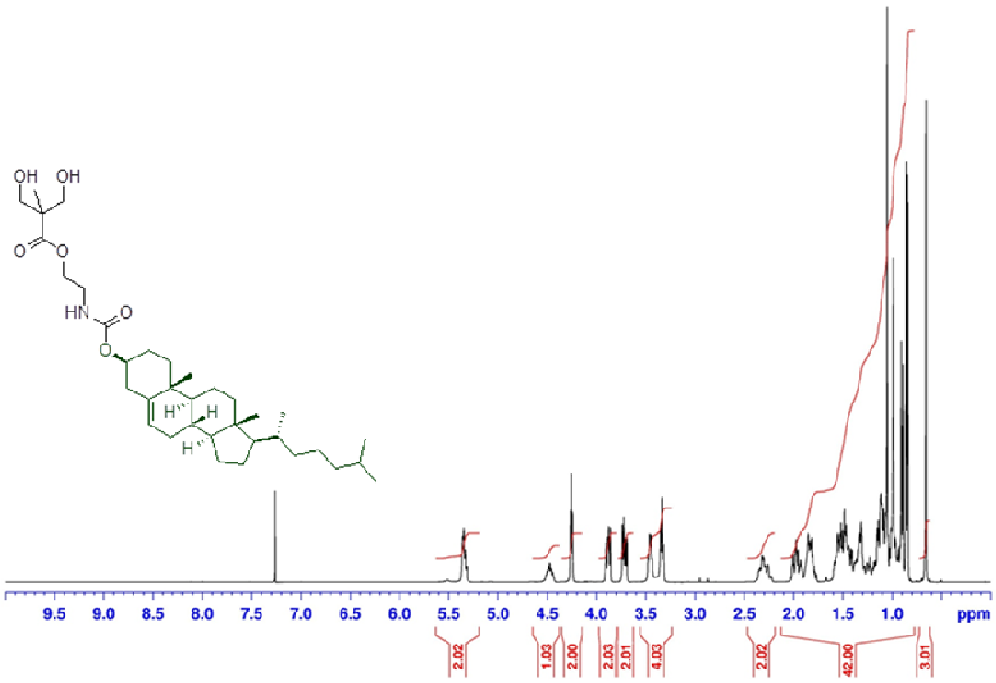

Figure 5S: ^{1}H NMR spectrum of **2** in $CDCl_3$

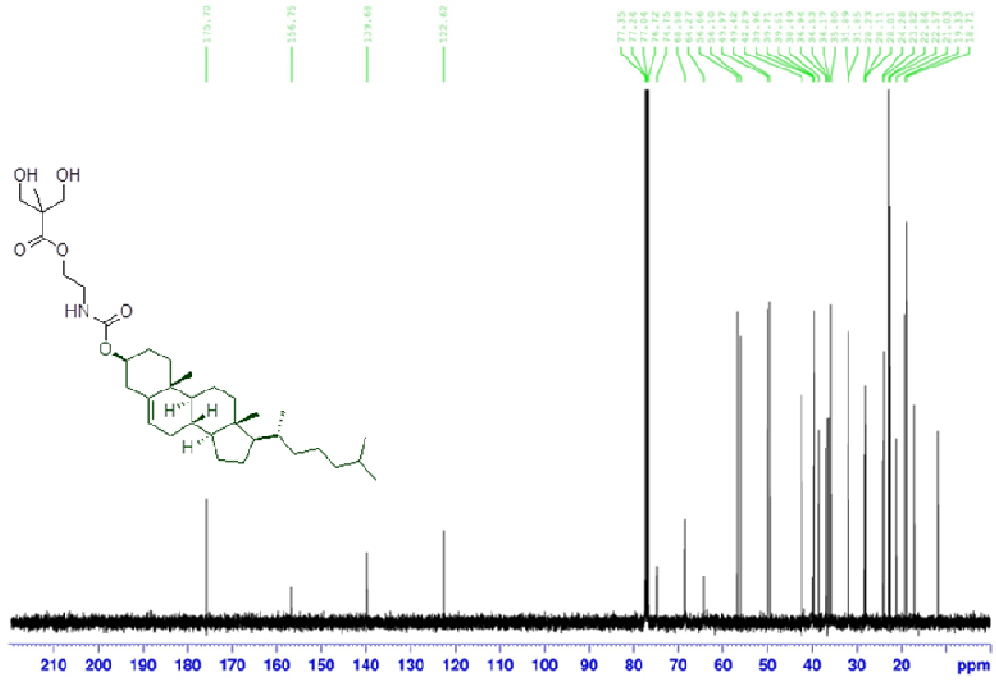

Figure 6S: ^{13}C NMR spectrum of **2** in $CDCl_3$

Instrument / Ser# micrOTOF-Q II 10269

Acquisition Parameter

Source Type	ESI	Ion Polarity	Positive	Set Nebulizer	2.0 Bar
Focus	Not active	Set Capillary	4500 V	Set Dry Heater	150 °C
Scan Begin	50 m/z	Set End Plate Offset	-500 V	Set Dry Gas	5.0 l/min
Scan End	1000 m/z	Set Collision Cell RF	120.0 Vpp	Set Divert Valve	Waste

Meas. m/z	#	Formula	m/z	err [ppm]	rdb	e⁻ Conf	N-Rule
612.4257	1	C 35 H 59 N Na O 6	612.4235	-3.7	6.5	even	ok
	2	C 37 H 58 N O 6	612.4259	0.2	9.5	even	ok

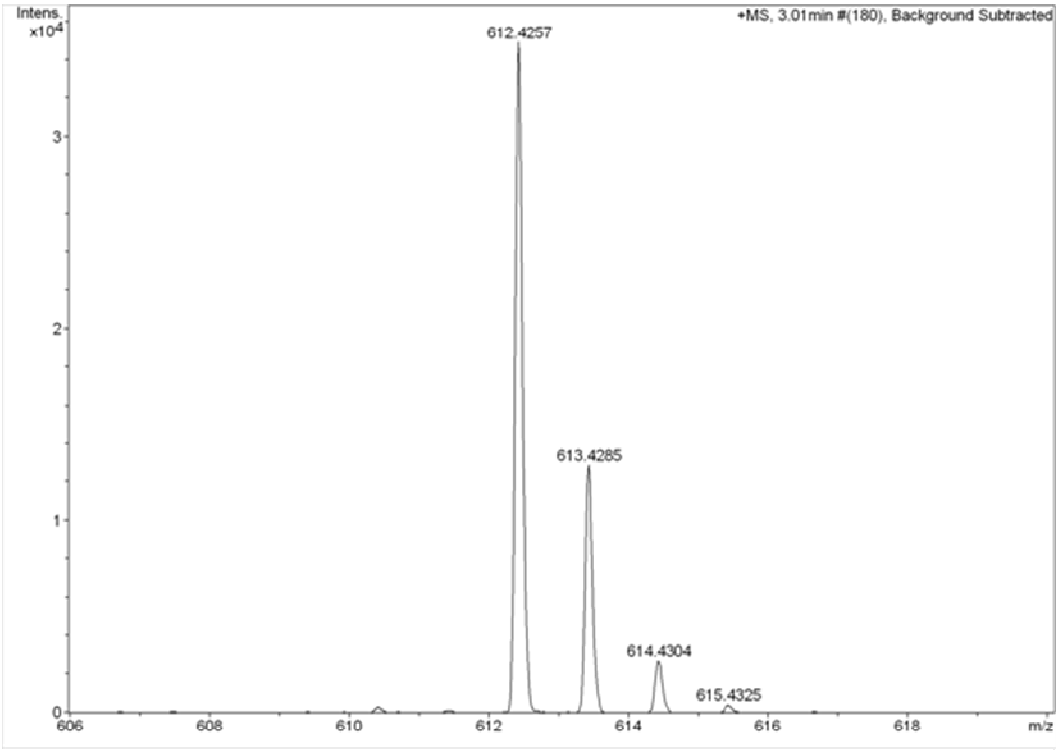

Figure 7S: HRMS spectrum of **2**

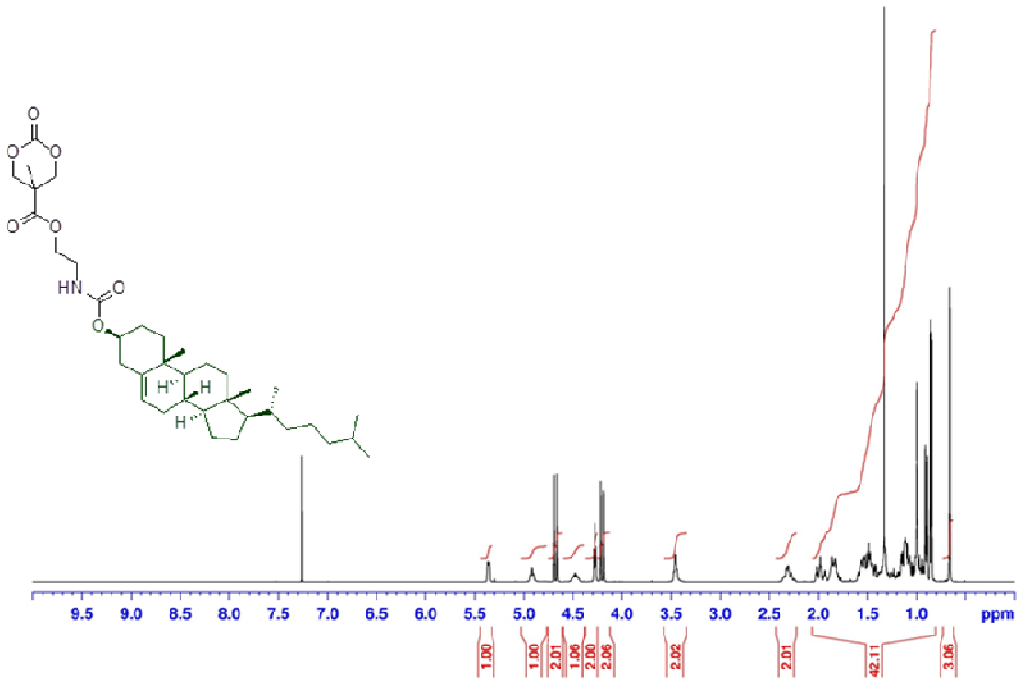

Figure 8S: ^{1}H NMR spectrum of **3** in $CDCl_3$

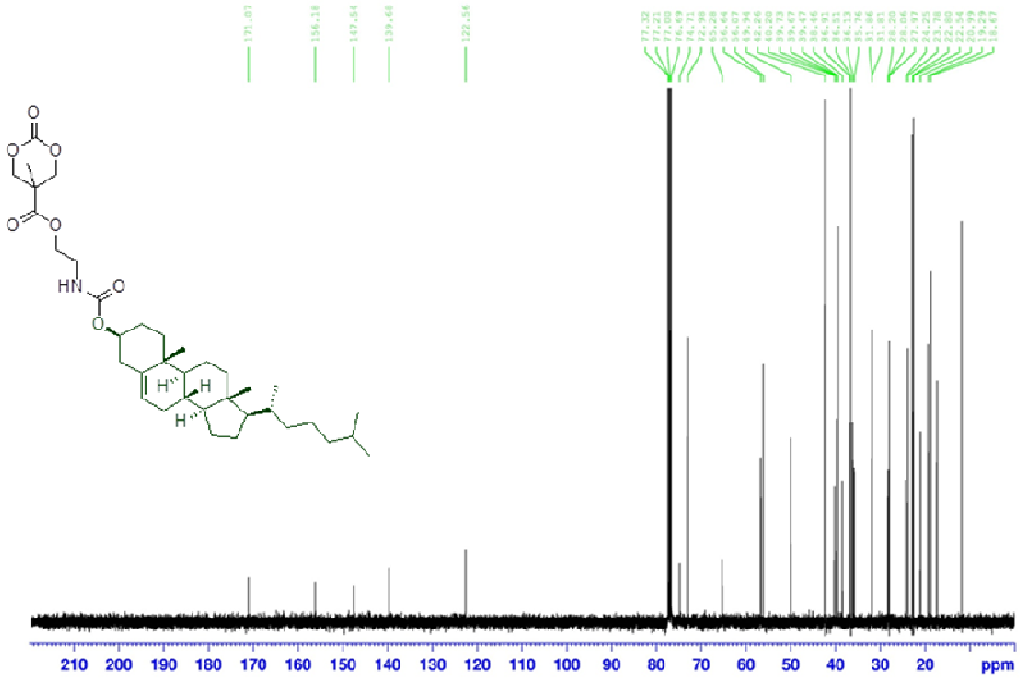

Figure 9S: ^{13}C NMR spectrum of **3** in $CDCl_3$

Instrument / Ser# micrOTOF-Q II 10269

Acquisition Parameter

Source Type	ESI	Ion Polarity	Positive	Set Nebulizer	2.0 Bar
Focus	Not active	Set Capillary	4500 V	Set Dry Heater	150 °C
Scan Begin	50 m/z	Set End Plate Offset	-500 V	Set Dry Gas	5.0 l/min
Scan End	1000 m/z	Set Collision Cell RF	120.0 Vpp	Set Divert Valve	Waste

Meas. m/z	#	Formula	m/z	err [ppm]	rdb	e⁻ Conf	N-Rule
638.4034	1	C 36 H 57 N Na O 7	638.4027	-1.1	8.5	even	ok
	2	C 38 H 56 N O 7	638.4051	2.7	11.5	even	ok

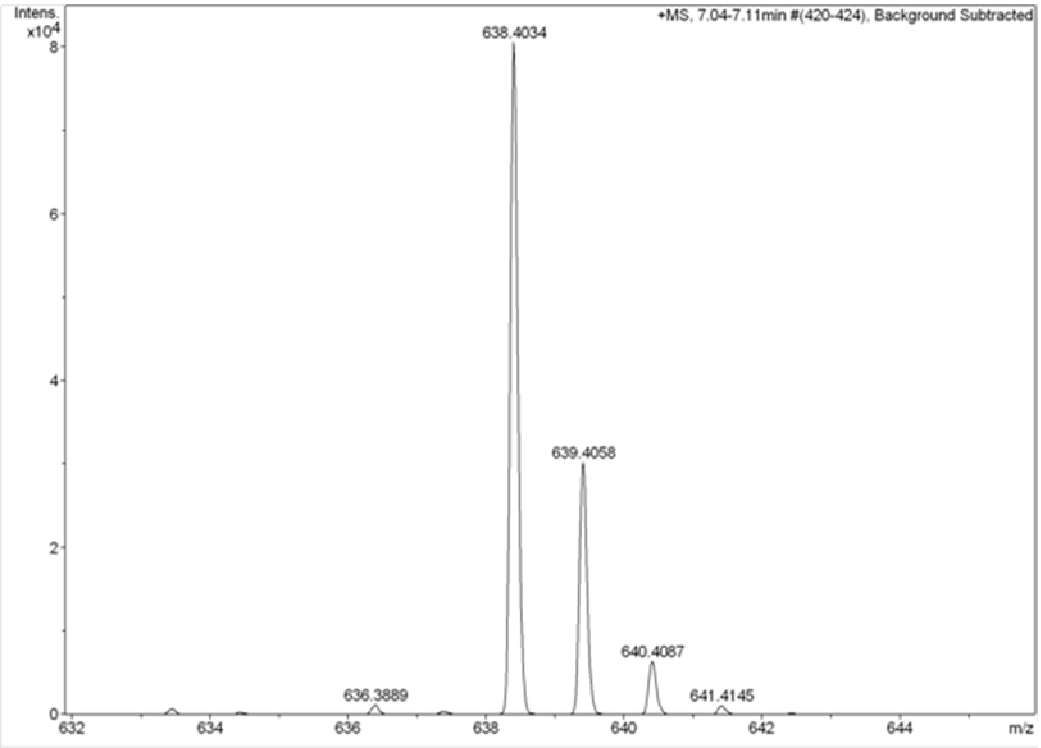

Figure 10S: HRMS spectrum of **3**

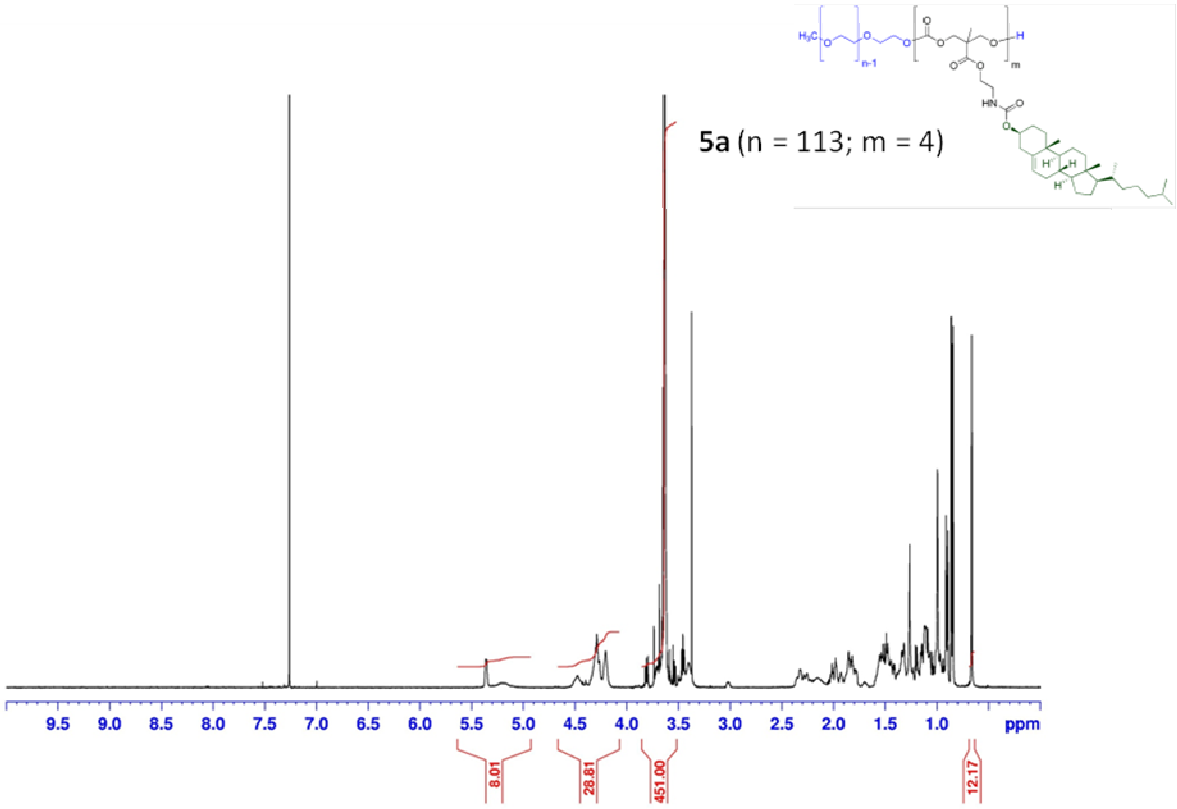

Figure 11S: ^{1}H NMR spectrum of **5a** in $CDCl_3$

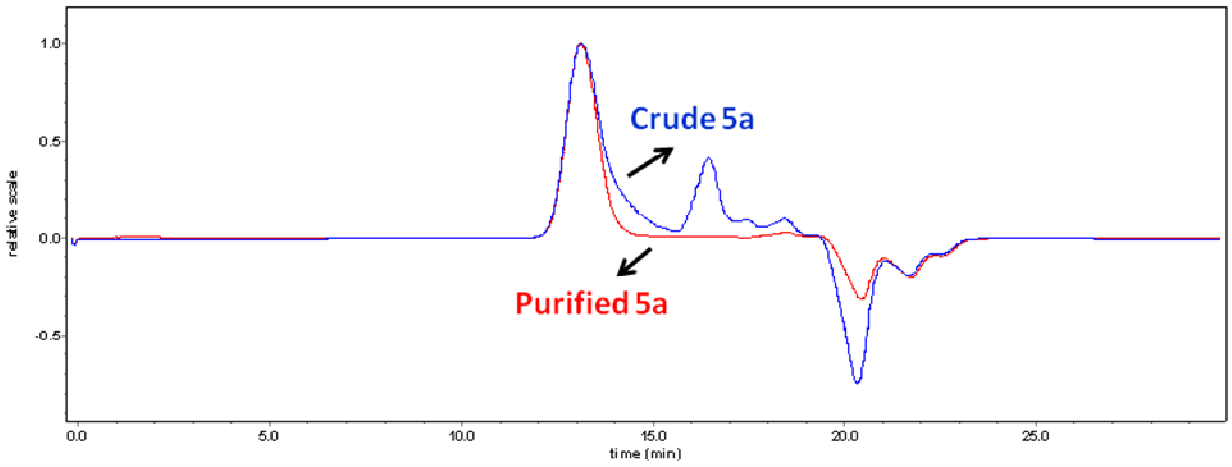

Figure 12S: Overlaid SEC chromatographs of crude and purified **5a**

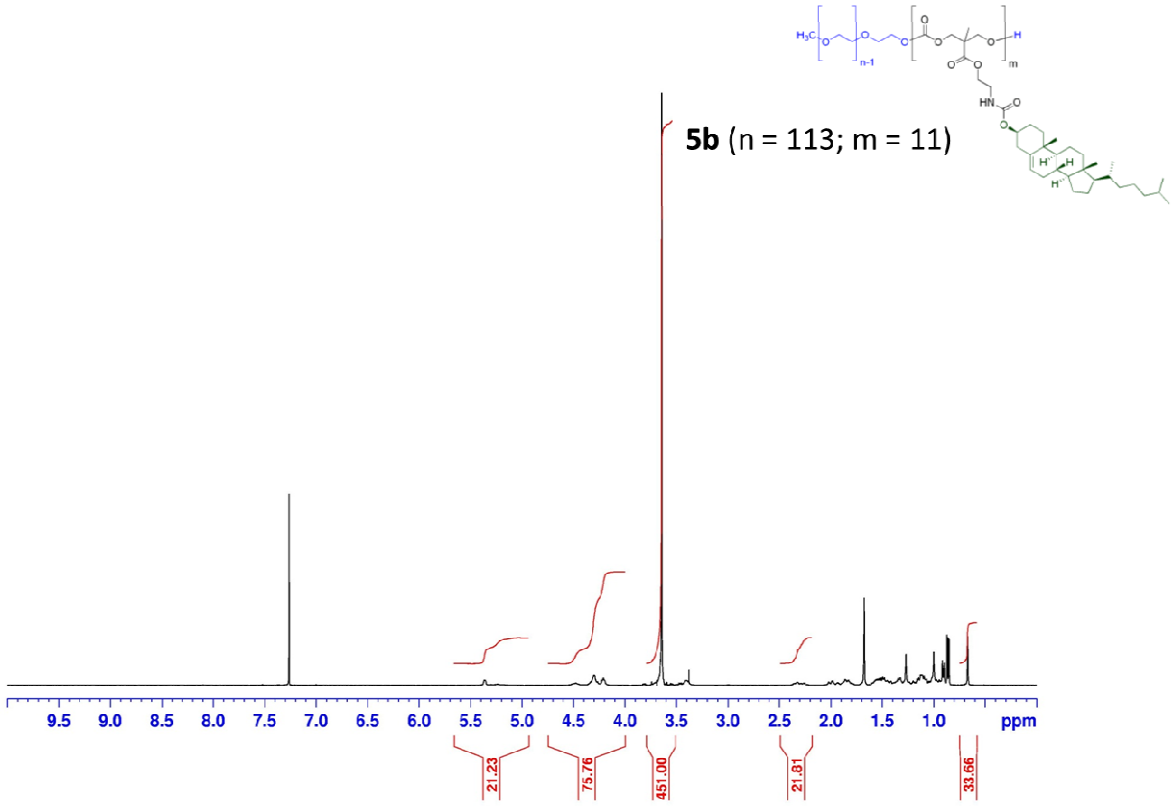

Figure 14S: ^{1}H NMR spectrum of **5b** in $CDCl_3$

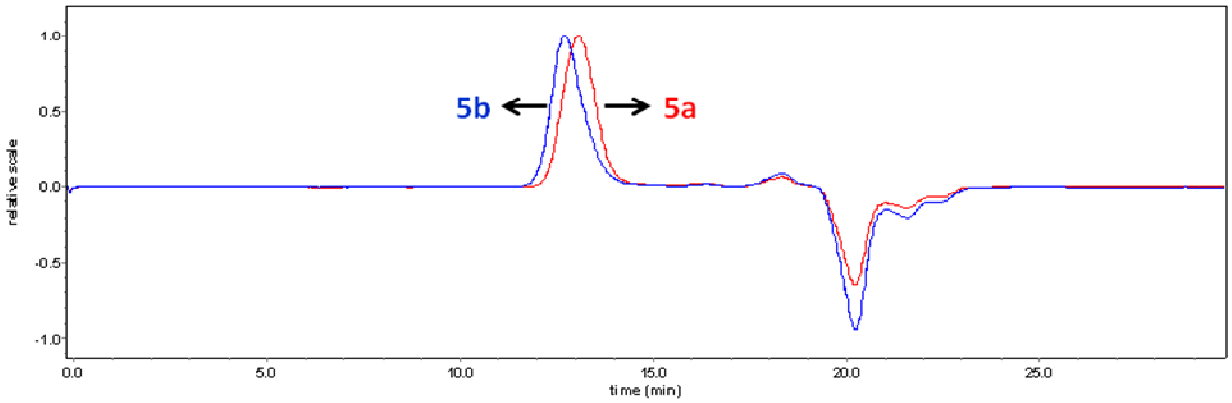

Figure 14S: Overlaid SEC chromatographs of purified **5a** and **5b**

§ Official contribution of the National Institute of Standards and Technology; not subject to copyright in the United States

‡Certain commercial equipment and materials are identified in this paper in order to specify adequately the experimental procedure. In no case does such identification imply recommendations by the National Institute of Standards and Technology nor does it imply that the material or equipment identified is necessarily the best available for this purpose

References

1. Pratt, R. C.; Lohmeijer, B. G. G.; Long, D. A.; Lundberg, P. N. P.; Dove, A. P.; Li, H.; Wade, C. G.; Waymouth, R. M.; Hedrick, J. L. *Macromolecules* **2006,** 39, 7863-7871.
2. Pedersen, J. S. *J Appl. Cryst.* **2000,** 33, 637-640.
3. Pedersen, J. S.; Svaneborg, C.; Almdal, K.; Hamley, I. W.; Young, R. N. *Macromolecules* **2003,** 36, 416-433.
4. Devanand, K.; Selser, J. C. *Macromolecules* **1991,** 94, 5943-5947.
5. Glatter, O.; Kratky, O., *Small-Angle X-ray Scattering*. Academic Press: London, 1982.